Available online at www.sciencedirect.com
ScienceDirect
Journal of Magnetic Resonance 189 (2007) 32–37
JMR Journal of Magnetic Resonance
www.elsevier.com/locate/jmr

Assessing signal enhancement in distant dipolar field-based sequences

Wilson Barros Jr. *, Daniel F. Gochberg, John C. Gore

Vanderbilt University Medical Center, Institute of Imaging Science (VUIIS), AA-1105 MCN, Nashville, TN 37232-2310, USA

Received 22 June 2007; revised 17 August 2007
Available online 29 August 2007

Abstract

The possibility of improving the signal-to-noise efficiency of NMR signal refocused by long-range dipolar interactions has been discussed recently [R.T. Branca, G. Galiana, W.S. Warren, Signal enhancement in CRAZED experiments, J. Magn. Reson. 187 (2007) 38–43]. For systems where $T_1 \gg T_2$, by including an extra radio-frequency pulse in a standard CRAZED sequence, it is possible to increase the available signal by exploiting its sensitivity to T_1 relaxation. Here, we use analytical calculations to investigate the source of this improved signal and determine the maximum enhancement provided by the method.

Keywords: Distant dipolar field; Intermolecular multiple-quantum coherences; Stimulated echo; Long-range dipolar interactions; Signal enhancement; CRAZED

1. Introduction

The NMR signal refocused in the presence of long-range dipolar interactions, also known as distant dipolar field (DDF) interactions, is related to the observation of intermolecular multiple-quantum coherences (iMQC). This signal exhibits very unusual properties and has found applications in high resolution spectroscopy and imaging [1,2]. A more general utilization of DDF-related effects is prevented by the poor signal-to-noise efficiency inherent to current methodologies. Several methods have been suggested recently for improving the signal-to-noise ratio in DDF-based sequences [3–5]. One of these methods [5] exploits signal sensitivity to T_1 relaxation by applying an extra pulse in a standard CRAZED sequence (see Fig. 1). Apparently when the T_1 spin–lattice relaxation occurs in a time-scale much longer than the T_2 spin–spin relaxation, which is the case in several biologically important systems, the T_2-dependent transverse magnetization can be partially replaced by some of the T_1-dependent longitudinal magnetization in a ''stimulated-echo-like'' approach [6] thereby providing some enhancement in the observed signal. Simulation results and experiments [5] corroborate this idea but the detailed mechanism of this enhancement and its maximum value are yet to be determined.

Here we investigate this effect analytically by solving the modified Bloch–Torrey equations where the DDF contribution is included via a mean-field theory approximation. Assuming T_2 relaxation as the principal attenuation mechanism, the effect of diffusion in the transverse magnetization as well as contributions from higher order terms in a Bessel function expansion can be neglected. With this assumptions we are able to obtain an approximate solution that accounts for the enhanced signal effect and allows for evaluating the maximum enhancement available from this method.

2. Theory

The detection of iMQCs in liquids is based on the idea that the existence of a modulation helix in the magnetization can break the angular-symmetry of the dipolar interaction and recover the long-range part of the motionally averaged dipolar field between spins in separate molecules [7]. This long-range dipolar field is responsible for converting the

* Corresponding author. Fax: +1 615 322 0734.
E-mail address: wilson.barros@vanderbilt.edu (W. Barros Jr.).

1090-7807/$ - see front matter © 2007 Elsevier Inc. All rights reserved.
doi:10.1016/j.jmr.2007.08.015

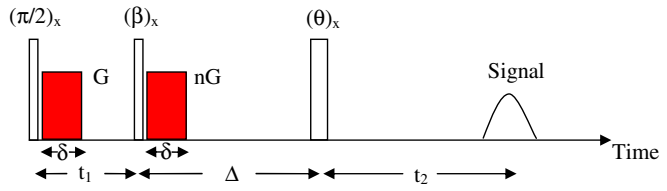

Fig. 1. Modified CRAZED pulse sequence where a third pulse θ was included in order to enhance DDF refocused signal. (The time-intervals are not in scale.)

iMQCs into observable signal. The theoretical framework for evaluating the detected signal follows two conceptually different views: the quantum [8] and the classical approach [9], which have proven to give the same results at least for non-confining geometries [10]. The classical approach, where the effect of the dipolar field interactions are considered, via a mean-field theory, as a non-linear additional term in the Bloch–Torrey equations is commonly adopted since it offers a straightforward approach to quantitative results. In a frame rotating at the Larmor frequency of a single species of spin, with gyromagnetic ratio γ, and assuming that radio-frequency (RF) inhomogeneities and background gradients can be neglected

$$\frac{\partial M^+}{\partial t} = -\mathrm{i}\gamma[\mathbf{G}\cdot\mathbf{r} + B_{dz}(r,t)]M^+ - \frac{M^+}{T_2} + D\nabla^2 M^+,$$
$$\frac{\partial M_z}{\partial t} = -\frac{M_z - M_0}{T_1} + D\nabla^2 M_z, \qquad (1)$$

where the transverse magnetization density $M^+ \equiv M_x + \mathrm{i}M_y$, and M_0 denotes the uniform thermal equilibrium magnetization density. $\mathbf{G}$ is an externally applied gradient used to break the dipolar interaction angular-symmetry, $B_{dz}(r,t)$ is the DDF component along the z-direction, and since $\mathbf{M}\times\mathbf{M} = 0$ there are no transverse contributions of $B_d(r,t)$ to be considered in the z-magnetization dynamics. T_2 and T_1 are, respectively, the spin–spin and spin–lattice relaxation times.

Analytical expressions for $B_{dz}(r,t)$ can be obtained in special cases, e.g., when the magnetization is sinusoidally modulated along a single direction $\hat{s}$ with $k_m L \gg 1$, where L is the sample smallest dimension. $k_m = \gamma G\delta$ denotes the wave vector of spatial modulation magnetization caused by the magnetic field gradient G applied during an interval δ. Under these conditions, assuming the polarizing field along the z-axis, the z component of the distant dipolar field can be written in its local form as $B_{dz}(r,t) = -\mu_0 \Delta_s M_z(s,t)$, where $\Delta_s = (3\cos^2\phi - 1)/2$ with $s = \hat{\mathbf{s}}\cdot\mathbf{r}$. μ_0 is the vacuum permeability and ϕ is the angle between the polarizing field direction $\hat{z}$ and the modulating gradient direction $\hat{s}$. In a more general scenario an analytic expression for the DDF is not possible and numerical treatments will be required. However, the effects studied here are related to relaxation time sensitivities that are independent from the DDF exact form. Thus, making use of the local form of the DDF in the following calculations is not a restriction for the final results.

Here we will be interested in the regime where the T_2 spin–spin relaxation dominates the attenuation process. Under this regime it is safe to neglect any effect of diffusion on M^+. If diffusion attenuation is considered only in the z-magnetization component, the modified Bloch–Torrey equations can be solved analytically. After the application of the first $(\pi/2)_x$ pulse and the gradient pulse of area $G\delta$ along a direction $\hat{s}$ as described in Fig. 1, the magnetization density becomes $M^+(r,\delta) = \mathrm{i}M_0\exp(-\mathrm{i}k_m s)$ and $M_z = 0$. (Here we consider that the gradients modulate the magnetization instantaneously.) This magnetization helix is attenuated at later times by relaxation and diffusion which are ignored during the RF and gradient pulses. Following the magnetization after the first 90° pulse and considering the expression for $B_{dz}(r,t)$ in its local form, after the second RF pulse β and immediately after the second gradient pulse (see Fig. 1) the magnetization is

$$M^+(r,t_1+\delta) = \mathrm{i}\frac{M_0}{2}\mathrm{e}^{-(t_1+\delta)/T_2}\times\left[(\cos\beta+1)\mathrm{e}^{-\mathrm{i}(n+1)k_m s} + (\cos\beta-1)\mathrm{e}^{-\mathrm{i}(n-1)k_m s}\right],$$
$$M_z(r,t_1+\delta) = -M_0\mathrm{e}^{-(t_1+\delta)/T_2}\sin\beta\cos k_m s. \qquad (2)$$

The magnetization along the z-direction generates the distant dipolar field that will refocus signal. The transverse magnetization that relaxes back to the z-direction during t_1 is negligible if $T_1 \gg t_1$ and will be discarded hereafter. During the interval Δ the signal evolves in the presence of the DDF as given below:

$$\begin{aligned} M^+(r,t_1+\Delta) &= M^+(r,t_1)\mathrm{e}^{-\Delta/T_2}\exp\left(-\mathrm{i}\gamma\int_{t_1}^{\Delta} B_{dz}(r,t)\mathrm{d}t\right)\\ &= M^+(r,t_1)\mathrm{e}^{-\Delta/T_2}\exp(\mathrm{i}\xi_1(\Delta)\cos k_m s)\\ &= M^+(t_1)\mathrm{e}^{-\Delta/T_2}\sum \mathrm{i}^l J_l(\xi_1(\Delta))\mathrm{e}^{\mathrm{i}lk_m s}\\ &= \mathrm{i}\frac{M_0}{2}\mathrm{e}^{-(t_1+\Delta)/T_2}\{J_0(\xi_1(\Delta))\left[(\cos\beta+1)\mathrm{e}^{-\mathrm{i}(n+1)k_m s}\right.\\ &\quad\left.+(\cos\beta-1)\mathrm{e}^{-\mathrm{i}(n-1)k_m s}\right]+\mathrm{i}^{n+1}J_{n+1}(\xi_1(\Delta))(\cos\beta+1)\\ &\quad+\mathrm{i}^{n-1}J_{n-1}(\xi_1(\Delta))(\cos\beta-1)+\cdots\} \end{aligned} \qquad (3)$$

$\xi_1(\Delta) = \frac{\Delta_s}{\tau_d}\frac{\sin\beta}{Dk_m^2+1/T_1}\mathrm{e}^{-t_1/T_2}(1-\mathrm{e}^{-\left(Dk_m^2+1/T_1\right)\Delta})$ and we have ignored terms in $B_{dz}(r,t)$ that have no s-dependence since they will not refocus signal. $\tau_d = 1/\mu_0\gamma M_0$ denotes the characteristic dipolar time. The magnetization has on its exponential argument a sinusoidal spatial-dependence that is conveniently expanded in terms of Bessel harmonics via the relation $\exp(\mathrm{i}A\cos\alpha) = \sum_{l=-\infty}^{\infty}\mathrm{i}^l J_l(A)\mathrm{e}^{\mathrm{i}l\alpha}$. In a standard CRAZED sequence when the spatial average of the magnetization over the sample volume is performed, from the infinite number of terms in the Bessel expansion, only terms independent of position, $l = n+1$ or $l = n-1$ in the expression above, produce observable signal. It turns out though that following an extra RF pulse, part of these dephased terms can be refocused thanks to the new DDF field during the interval after the additional pulse. For instance, the term $l = 0$ was kept in Eq. (3) and will be refocused during the t_2 interval by the action of the $l' = \pm 1$

Bessel harmonic contributions from the DDF that carry $e^{\pm ik_m s}$ spatial-dependence. Careful inspection of the myriad of terms that can be observed after the θ pulse shows that contributions from higher order Bessel harmonics combinations $J_l(\xi(\Delta))J_{l'}(\xi(t_2))$, where $l+l'>1$, give negligible contribution under strong T_2 relaxation. These terms will be discarded in the following calculations. The magnetization immediately after the θ pulse for $n=\pm 2$ yields

$$\begin{aligned} M^{+}_{n\pm 2}(r,t_1+\Delta+t_2') &= i\frac{M_0}{2}e^{-(t_1+\Delta)/T_2}\{J_0(\xi_1(\Delta))(\cos\beta\mp 1)\\ &\quad\times[\cos\theta\cos k_m s-\sin k_m s]+iJ_1(\xi_1(\Delta))(\cos\beta\mp 1)\}\\ &\quad- iM_0e^{-t_1/T_2}e^{-\left(Dk_m^2+1/T_1\right)\Delta}\sin\beta\sin\theta\cos k_m s, \end{aligned} \tag{4}$$

$$\begin{aligned} M_{z(n\pm 2)}(r,t_1+\Delta+t_2') &= -M_0\left[e^{-t_1/T_2}e^{-\left(Dk_m^2+1/T_1\right)\Delta}\sin\beta\cos\theta\right.\\ &\quad\left.+\frac{1}{2}e^{-(t_1+\Delta)/T_2}J_0(\xi_1(\Delta))(\cos\beta\mp 1)\sin\theta\right]\cos k_m s, \end{aligned} \tag{5}$$

where t_2' is the instant immediately after the θ pulse. For the case $n=0$:

$$\begin{aligned} M^{+}_{n=0}(r,t_1+\Delta+t_2') &= \frac{M_0}{2}e^{-(t_1+\Delta)/T_2}\{iJ_0(\xi_1(\Delta))[\cos\beta\cos\theta\cos k_m s+\sin k_m s]\\ &\quad-J_1(\xi_1(\Delta))\cos\beta\}-iM_0e^{-t_1/T_2}e^{-\left(Dk_m^2+1/T_1\right)\Delta}\sin\beta\sin\theta\cos k_m s, \end{aligned} \tag{6}$$

$$\begin{aligned} M_{z(n=0)}(r,t_1+\Delta+t_2') &= -M_0\left[e^{-t_1/T_2}e^{-\left(Dk_m^2+1/T_1\right)\Delta}\sin\beta\cos\theta\right.\\ &\quad\left.+e^{-(t_1+\Delta)/T_2}J_0(\xi_1(\Delta))\cos\beta\sin\theta\right]\cos k_m s. \end{aligned} \tag{7}$$

During the t_2 interval for either $n=0$ or $n=\pm 2$ the DDF field, given, respectively, by Eqs. (5) and (7), will refocus the magnetization described by Eqs. (4) and (6). The process is similar to the one described in Eq. (3) and yields

$$\begin{aligned} \overline{M^{+}_{n=0}(t_1+\Delta+t_2)} &= -M_0e^{-(t_1+t_2)/T_2}\left\{e^{-\Delta/T_2}\left[\cos\beta\cos\theta J_0(\xi_1(\Delta))J_1\left(\xi_2^0(t_2)\right)\right.\right.\\ &\quad\left.\left.+\cos\beta J_1(\xi_1(\Delta))J_0\left(\xi_2^0(t_2)\right)\right]+e^{-\left(Dk_m^2+1/T_1\right)\Delta}\sin\beta\sin\theta J_1\left(\xi_2^0(t_2)\right)\right\}, \end{aligned} \tag{8}$$

$$\begin{aligned} \overline{M^{+}_{n=+2}(t_1+\Delta+t_2)} &= -\frac{M_0}{2}e^{-(t_1+t_2)/T_2}\left\{e^{-\Delta/T_2}(\cos\beta-1)\left[\cos\theta J_0(\xi_1(\Delta))J_1\left(\xi_2^{+2}(t_2)\right)\right.\right.\\ &\quad\left.\left.+J_1(\xi_1(\Delta))J_0\left(\xi_2^{+2}(t_2)\right)\right]+2e^{-\left(Dk_m^2+1/T_1\right)\Delta}\sin\beta\sin\theta J_1\left(\xi_2^{+2}(t_2)\right)\right\}, \end{aligned} \tag{9}$$

$$\begin{aligned} \overline{M^{+}_{n=-2}(t_1+\Delta+t_2)} &= -\frac{M_0}{2}e^{-(t_1+t_2)/T_2}\left\{e^{-\Delta/T_2}(\cos\beta+1)\left[\cos\theta J_0(\xi_1(\Delta))J_1\left(\xi_2^{-2}(t_2)\right)\right.\right.\\ &\quad\left.\left.+J_1(\xi_1(\Delta))J_0\left(\xi_2^{-2}(t_2)\right)\right]+2e^{-\left(Dk_m^2+1/T_1\right)\Delta}\sin\beta\sin\theta J_1\left(\xi_2^{-2}(t_2)\right)\right\}, \end{aligned} \tag{10}$$

where the overline means spatial average over the sample and the DDF contributions for $n=0$ and $n=\pm 2$ are, respectively,

$$\begin{aligned} \xi_2^0(t_2) &= \frac{\Delta_s}{\tau_d}\left[e^{-t_1/T_2}e^{-\left(Dk_m^2+1/T_1\right)\Delta}\sin\beta\cos\theta\right.\\ &\quad\left.+e^{-(t_1+\Delta)/T_2}J_0(\xi_1(\Delta))\cos\beta\sin\theta\right]\\ &\quad\times\frac{1}{Dk_m^2+1/T_1}\left(1-e^{-\left(Dk_m^2+1/T_1\right)t_2}\right), \end{aligned} \tag{11}$$

$$\begin{aligned} \xi_2^{\pm 2}(t_2) &= \frac{\Delta_s}{\tau_d}\left[e^{-t_1/T_2}e^{-\left(Dk_m^2+1/T_1\right)\Delta}\sin\beta\cos\theta\right.\\ &\quad\left.+\frac{1}{2}e^{-(t_1+\Delta)/T_2}J_0(\xi_1(\Delta))(\cos\beta\mp 1)\sin\theta\right]\\ &\quad\times\frac{1}{Dk_m^2+1/T_1}\left(1-e^{-\left(Dk_m^2+1/T_1\right)t_2}\right). \end{aligned} \tag{12}$$

3. Results and discussion

The parameters $\tau_d=240$ ms, $T_2=50$ ms and $T_1=1$ s were utilized in all calculations and the gradients were considered parallel ($\hat{s}||\hat{z}$) with the B_0 field ($\Delta_s=1$) in order to provide a comparison with previous simulated results from the literature [5].

Fig. 2 shows curves where the absolute value of the analytical solution of the modified Bloch-equations for the cases $n=0$ (see Eq. (8)) and $n=+2$ (see Eq. (9)) are plotted as a function of the interval t_2 (see Fig. 1). Curves were plotted for values of the Δ interval varying from 10 to 50 ms for the case of no diffusion. The maximum signal is obtained with $\Delta=40$ ms using the parameters given in the caption. In both cases the maximum signal-peak obtained is higher than that obtained by the maximum signal available by conventional CRAZED sequence represented by the dashed lines in each panel [11]. The maximum signal for the cases $n=0$ and $n=+2$, when compared to the corresponding standard CRAZED maximum signal, show an enhancement of 15% and 10%, respectively. Furthermore, in a conventional CRAZED sequence, in the regime where T_2 relaxation is the dominant attenuation process, the maximum refocused signal occurs at $\Delta+t_2=T_2$ which is 50 ms in the case described. As such, one would expect the maximum signal for the modified sequence to be given by a similar relation. In fact, the results indicate that the maximum signal does not necessarily occurs at that point. For instance, for the case of $T_2=50$ ms, the maximum signal for the modified sequence was obtained at $\Delta+t_2\approx 60$ ms.

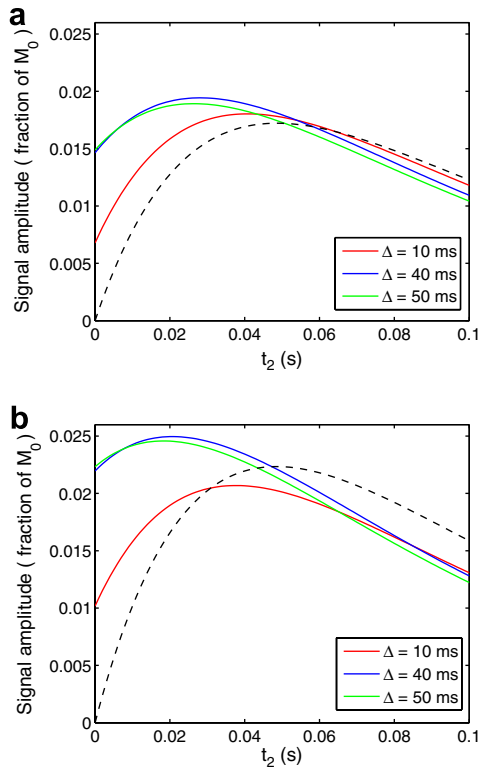

Fig. 2. Absolute value of DDF signal, given by Eq. (8) for $n = 0$ (panel a) and by Eq. (9) for $n = +2$ (panel b), as a function of the t_2 interval (see Fig. 1). The curves were plotted for different Δ neglecting the effect of diffusion. The parameters used were: $\beta = 120°$, $\theta = 25°$, $T_2 = 50$ ms, $T_1 = 1$ s, $\tau_d = 240$ ms, and $t_1 = 2$ ms. The dashed lines on each panel represent the signal obtainable using a conventional CRAZED sequence ($\theta = 0$, $\Delta = 0$ in Fig. 1) where $\beta = 45°$ for $n = 0$ and $\beta = 120°$ for $n = +2$.

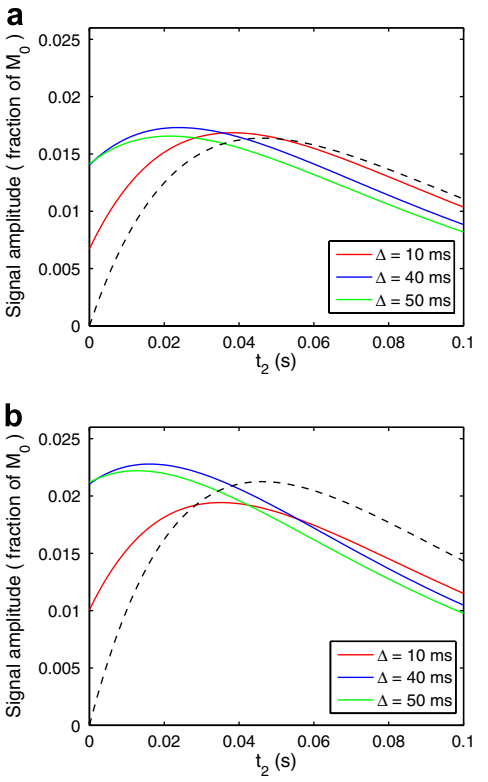

Fig. 3. Absolute value of DDF signal, given by Eq. (8) for $n = 0$ (panel a) and by Eq. (9) for $n = +2$ (panel b), as a function of the t_2 interval (see Fig. 1). The curves were plotted for different Δ using $1/Dk_m^2 = 464$ ms. The parameters used were: $\beta = 120°$, $\theta = 25°$, $T_2 = 50$ ms, $T_1 = 1$ s, $\tau_d = 240$ ms, and $t_1 = 2$ ms. The dashed lines on each panel represent the signal obtainable using a conventional CRAZED sequence ($\theta = 0$, $\Delta = 0$ in Fig. 1) where $\beta = 45°$ for $n = 0$ and $\beta = 120°$ for $n = +2$.

In Fig. 3 we consider the effects of diffusion in the longitudinal magnetization and the case with $1/Dk_m^2 = 464$ ms is presented. Again, the dashed lines indicate the result from the conventional CRAZED sequence. The effect of diffusion attenuation as seen in the analytical results can be understood as an effective T_1 relaxation. So, if $(1/T_1 + Dk_m^2)$ increases approaching $1/T_2$ the enhancement is reduced which indicates that the magnetization that evolved in the z-direction during Δ, given by the last term in Eqs. (7)–(9), is responsible for the improved signal.

Fig. 4 shows maps of the absolute signal-amplitude for the case $n = 0$ as a function of the pulse-angles β and θ for different values of the Δ interval. The maximum signal can then be calculated and, for $\Delta = 30$ ms, is up to 15% higher than the original CRAZED-sequence signal. Apart from the overall change in the maps appearance as a function of Δ, the areas where the signal reaches a maximum are rather stable.

Fig. 5 shows maps of the absolute signal-amplitude for the case $n = +2$ in the same way as described for Fig. 4. The maximum signal is up to 10% higher than the original CRAZED-sequence signal for $\Delta = 40$ ms. Again, besides the overall change in the maps appearance as a function of Δ, the areas where the signal reaches a maximum are rather stable. The case for $n = -2$ is not shown but overall produces enhancement similar to the $n = +2$ except for the differences in the combinations of β and θ angles.

4. Summary

Analytical calculations for the distant dipolar field refocused signal in a modified CRAZED sequence have been presented. For systems where T_2 relaxation is the main source of signal attenuation, diffusion effects can be neglected in the transverse magnetization. This allows for a closed-form analytical solution based on the Bloch–Torrey equations modified to include the distant dipolar field contribution and considering the role of diffusion on the longitudinal magnetization. This is a good approximation if $1/Dk_m^2 \gg T_2$. For more general regimes analytic solutions including diffusion turn out to be complicated [12]. The solution presented here, valid if $(t_2 + \Delta) \approx T_2 \ll \tau_d$, neglects terms coming from combinations of Bessel function contributions of added order higher than one.

Given some specific sample parameters, a maximum signal enhancement up to 15% of the signal available from a conventional CRAZED sequence was obtained for the sequence depicted in Fig. 1 with either $n = 0$ or $n = \pm 2$. Similar enhancement was found (data not shown) for other

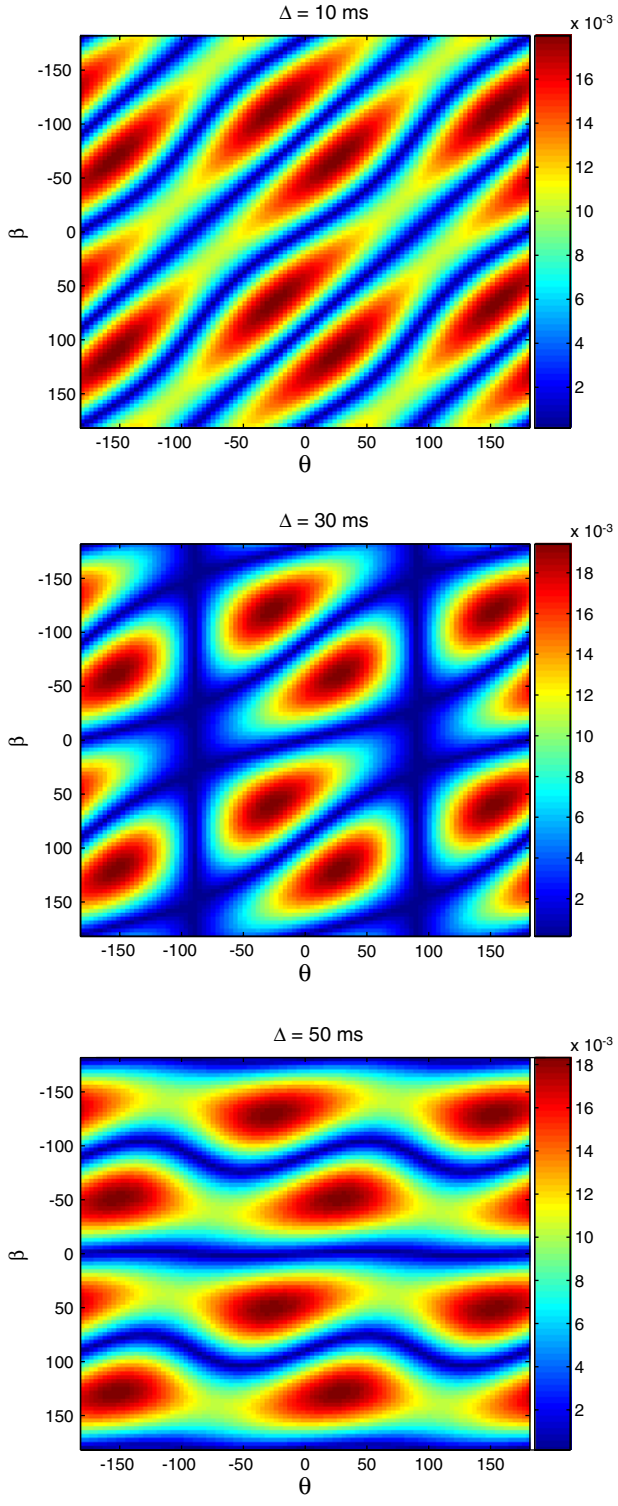

Fig. 4. DDF refocused signal for the case $n = 0$ considering no diffusion. The intensity maps as a function of β and θ obtained from the absolute value of $\overline{M^{+}_{n=0}(t_2)}$ in Eq. (8): $T_2 = 50$ ms, $T_1 = 1$ s, $t_1 = 2$ ms and $(\Delta + t_2) = 60$ ms. The values of Δ are indicated on top of each panel. The best enhancement, around 15%, was obtained for peaks on the panel $\Delta = 30$ ms.

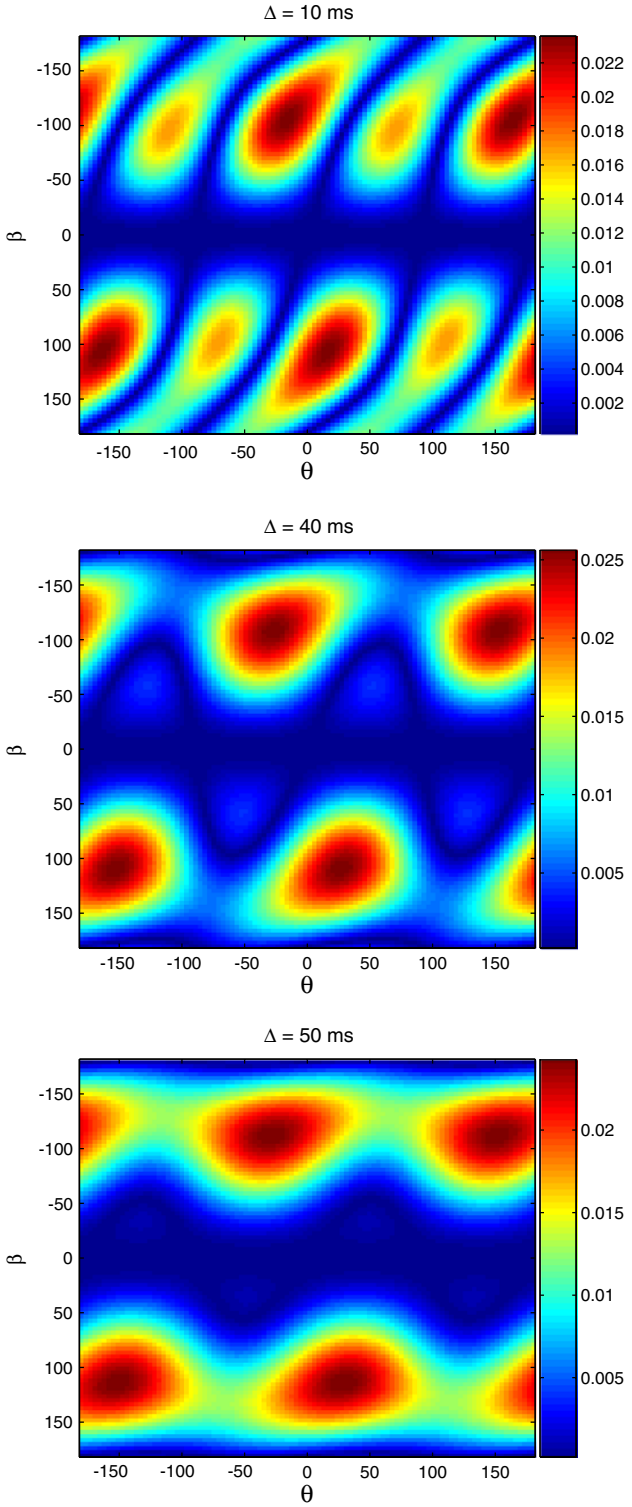

Fig. 5. DDF refocused signal for the case $n = +2$ considering no diffusion. The intensity maps as a function of β and θ obtained from the absolute value of $\overline{M^{+}_{n=+2}(t_2)}$ in Eq. (9): $T_2 = 50$ ms, $T_1 = 1$ s, $t_1 = 2$ ms and $(\Delta + t_2) = 60$ ms. The values of Δ are indicated on top of each panel. The best enhancement, around 10%, was obtained for peaks on the panel $\Delta = 40$ ms.

parameter data-sets in the regime $T_1 \gg \tau_d > T_2$. The results generally agree with the numerical data given in reference [5] with a few minor discrepancies [13]. We have not considered effects of the background gradient generated by the polarizing B_0 field. Thus, to reproduce experimentally the results calculated here, 180° refocusing pulses have to

be symmetrically inserted within each time-interval of the sequence in Fig. 1. The imaging case has to be taken carefully since encoding gradients during the t_1 interval affect the DDF. Thus it is wise to perform the imaging encoding during the time immediately before acquiring the signal where the DDF is pointing along the polarizing field and will not be affected by these gradients.

Phase cycling strategies for cancelling out potential spurious signal were not investigated. Along these lines, there might be some concern that the signal generated with the modified CRAZED sequence could originate from single-quantum coherence pathways [14]. However, if the effect of the DDF is neglected there is no observable signal which indicates that the signal originates from dipolar interactions. Nevertheless, it should be mentioned that similar modifications in standard CRAZED sequences have proved recently to be more robust to pulse angle imperfections [15,16].

This modified CRAZED sequence is intended to benefit from T_1-sensitive signal contribution for systems where $T_1 \gg T_2$ with negligible effect of diffusion. The results show that diffusion effects may minimize the enhancement available even if $T_1 \gg T_2$. The small increase in the signal, up to 15% in the best scenario, contrasts with the much higher signal enhancement available in standard single-quantum methods. For instance, in a Hahn-stimulated-echo experiment, the signal is attenuated exclusively by T_1 relaxation. This is possible because the longitudinal signal is immediately available for observation when flipped into the transverse plane which mitigates the effect of T_2 relaxation. On the other hand, for the DDF signal, although the longitudinal part of the magnetization relaxes under T_1 effect during the Δ interval, after the θ pulse (see Fig. 1) this dephased magnetization needs some time (in the order of τ_d) in the transverse plane to build up in the presence of the DDF, thereby suffering from T_2 attenuation during this interval. One might think that going to higher field, where τ_d gets shorter, could alleviate this issue; however, at higher fields the signal-peak will appear in a time-scale independent of any relaxation time which makes the use of relaxation-dependent magnetization to improve signal meaningless.

Finally, the goal of this contribution was, via analytical calculations, to investigate the origin of the enhanced signal when an additional pulse is included in a standard CRAZED sequence and evaluate the maximum enhancement possible for this type of sequence implementation. Unfortunately, the way the NMR signal builds up in the presence of the DDF prevents an appreciable signal enhancement based on the more favorable T_1 sensitivity. Nevertheless, it should be pointed out that these conclusions do not rule out the possibility of using this method to obtain contrast enhancement in some properly designed experiment.

Acknowledgments

W. Barros thanks Dr. R.T. Branca for helpful clarifications about their work. This work was supported by NIH Grants No. R21 EB04040 and RO1 EB000214.

References

[1] S. Vathyam, S. Lee, W.S. Warren, Homogeneous NMR spectra in inhomogeneous fields, Science 272 (1996) 92–96.
[2] W.S. Warren, S. Ahn, M. Mescher, M. Garwood, K. Ugurbil, W. Richter, R.R. Rizi, J. Hopkins, J.S. Leigh, MR imaging contrast enhancement based on intermolecular zero quantum coherences, Science 281 (1998) 247–251.
[3] X. Zhu, S. Chen, Z. Chen, S. Cai, J. Zhong, Simultaneous acquisition and effective separation of intermolecular multiple-quantum signals of different orders, Chem. Phys. Lett. 438 (2007) 308–314.
[4] G. Galiana, R.T. Branca, W.S. Warren, Spin locking SQCs in an iMQC experiment, ENC conference abstract, 2006.
[5] R.T. Branca, G. Galiana, W.S. Warren, Signal enhancement in CRAZED experiments, J. Magn. Reson. 187 (2007) 38–43.
[6] I. Ardelean, R. Kimmich, Diffusion measurements using nonlinear stimulated echo, J. Magn. Reson. 101 (2000) 101–105.
[7] W.S. Warren, W. Richter, A.H. Andreotti, B.T. Farmer II, Generation of impossible cross-peaks between bulk water and biomolecules in solution NMR, Science 262 (1993) 2005–2009.
[8] S. Lee, W. Richter, S. Vathyam, W.S. Warren, Quantum treatment of the effects of dipole–dipole interactions in liquid nuclear magnetic resonance, J. Chem. Phys. 105 (1996) 874–900.
[9] G. Deville, M. Bernier, J.M. Delrieux, NMR multiple echoes observed in solid ^{3}He, Phys. Rev. B 119 (1979) 5666–5688.
[10] J. Jeener, Equivalence between the 'classical' and the 'Warren' approaches for the effects of long range dipolar couplings in liquid nuclear magnetic resonance, J. Chem. Phys. 112 (2000) 5091–5094.
[11] Z. Chen, S. Zheng, J. Zhong, Optimal RF flip angles for intermolecular multiple-quantum coherences of different orders with the CRAZED pulse sequence, Chem. Phys. Lett. 347 (2001) 143–148.
[12] W. Barros, J.C. Gore, D.F. Gochberg, NMR molecular diffusion in the presence of distant dipolar field interactions, ISMRM conference abstract, 2007.
[13] For the case $n = \pm 2$ there was some discrepancy in the maximum enhancement obtained here and that presented in reference [5]. Examining the conventional CRAZED maximum signal for the case ($n = +2$, $\beta = 120°$, $\theta = 0°$) and ($n = 0$, $\beta = 45°$, $\theta = 0°$) represented, respectively, by the dotted lines in Fig. 8 and Fig. 6 of reference [5], it was noticed that standard theoretical predictions for the ratio between these maxima was not respected which made a reasonable comparison with the analytical solution difficult. Furthermore, in the analytic results presented here, no signal enhancement was detected for $n = \pm 2$ if the second gradient was inserted after the θ pulse.
[14] Z. Chen, Z. Chen, J. Zhong, Observation and characterization of intermolecular homonuclear single-quantum coherences in liquid nuclear magnetic resonance, J. Chem. Phys. 117 (2002) 8426–8434.
[15] X. Zhu, Z. Chen, S. Cai, J. Zhong, Formation and identification of pure intermolecular zero-quantum coherence signal in liquid NMR, Chem. Phys. Lett. 421 (2006) 171–178.
[16] Z. Chen, X. Zhu, B. Zheng, S. Cai, J. Zhong, Double-quantum-filtered intermolecular single-quantum coherences in nuclear magnetic resonance spectroscopy and imaging, Chem. Phys. Lett. 429 (2006) 611–616.